Available online at www.sciencedirect.com
ScienceDirect
Journal of Power Sources 167 (2007) 151–161
JOURNAL OF POWER SOURCES
www.elsevier.com/locate/jpowsour

Analysis of the energy efficiency of an integrated ethanol processor for PEM fuel cell systems

Javier A. Francesconi, Miguel C. Mussati, Roberto O. Mato, Pio A. Aguirre *

INGAR – Instituto de Desarrollo y Diseño, Avellaneda 3657, CP: S3002GJC, Santa Fe, Argentina

Received 16 November 2006; received in revised form 21 December 2006; accepted 22 December 2006
Available online 6 February 2007

Abstract

The aim of this work is to investigate the energy integration and to determine the maximum efficiency of an ethanol processor for hydrogen production and fuel cell operation. Ethanol, which can be produced from renewable feedstocks or agriculture residues, is an attractive option as feed to a fuel processor. The fuel processor investigated is based on steam reforming, followed by high- and low-temperature shift reactors and preferential oxidation, which are coupled to a polymeric fuel cell. Applying simulation techniques and using thermodynamic models the performance of the complete system has been evaluated for a variety of operating conditions and possible reforming reactions pathways. These models involve mass and energy balances, chemical equilibrium and feasible heat transfer conditions (ΔT_{min}). The main operating variables were determined for those conditions. The endothermic nature of the reformer has a significant effect on the overall system efficiency. The highest energy consumption is demanded by the reforming reactor, the evaporator and re-heater operations. To obtain an efficient integration, the heat exchanged between the reformer outgoing streams of higher thermal level (reforming and combustion gases) and the feed stream should be maximized. Another process variable that affects the process efficiency is the water-to-fuel ratio fed to the reformer. Large amounts of water involve large heat exchangers and the associated heat losses.

A net electric efficiency around 35% was calculated based on the ethanol HHV. The responsibilities for the remaining 65% are: dissipation as heat in the PEMFC cooling system (38%), energy in the flue gases (10%) and irreversibilities in compression and expansion of gases. In addition, it has been possible to determine the self-sufficient limit conditions, and to analyze the effect on the net efficiency of the input temperatures of the clean-up system reactors, combustion preheating, expander unit and crude ethanol as fuel.

Keywords: Ethanol reforming; Hydrogen production; Fuel cells; Process integration

1. Introduction

In the last years, fuel cells have received a growing attention for power generation owing to their potential higher thermal efficiency and lower CO_2 emissions per unit of power produced.

Many research and development projects have been conducted on both the fuel cell itself and the fuel processors for generating hydrogen. There exist several routes for hydrogen production from the primary fuels. Ethanol presents several advantages related to natural availability, storage and handling safety; ethanol can be produced renewably from several biomass sources. In addition, the ethanol-to-hydrogen system has the significant advantage of being nearly CO_2 neutral, since the produced carbon dioxide is consumed for biomass growth, thus offering a nearly closed carbon loop [1].

Steam reforming [2–6] and autothermal reforming [7–9] are being considered as alternative processes for converting alcohols to hydrogen. The aim of this work is to investigate the energy integration of an ethanol fuel processor considering steam reforming coupled to a polymeric fuel cell. Proton exchange membrane (PEM) fuel cells for stationary applications are highly integrated systems, including the fuel processor, the fuel cell itself and the post-combustion unit [10,11]. Process design therefore has a great impact on the total system performance. The goal of this paper is to analyze and improve the fuel cell system (FCS) performance by simulation techniques. As a starting point for design, the hypothetical system proposed in Little [12] has been used as a reference case in

* Corresponding author. Tel.: +54 342 453 4451; fax: +54 342 455 3439.
E-mail addresses: javierf@ceride.gov.ar (J.A. Francesconi), mmussati@ceride.gov.ar (M.C. Mussati), rmato@ceride.gov.ar (R.O. Mato), paguir@ceride.gov.ar (P.A. Aguirre).

0378-7753/$ – see front matter © 2007 Elsevier B.V. All rights reserved.
doi:10.1016/j.jpowsour.2006.12.109

Nomenclature

E_{Rev}	reversible open circuit voltage (V)
E^0_{Rev}	reversible potential at standard pressure (V)
f^{FP}_{EtOL}	molar flow of ethanol to the reformer (kmol s^{-1})
f^{Bum}_{EtOL}	molar flow of ethanol to burn (kmol s^{-1})
F	Faraday constant (96,487 C mol^{-1})
l_{Cell}	cell current (A)
LHV_{EtOL}	lower heating value of ethanol (1235470 kJ kmol^{-1})
P_{Cell}	cell power (kW)
P_{Comp}	power compressor (kW)
P_{System}	net power produced by the fuel cell system (kW)
P_{Tur}	power expander (kW)
Q_{PEM}	heat generate from the fuel cell (kW)
Q_{Cooler}	heat to remove from the system (kW)
R	water to ethanol molar ratio
R_g	molar or 'universal' gas constant
T_{Ref}	reforming temperature (°C)
T_{Cell}	cell temperature (°C)
V_{Cell}	cell voltage (V)
W^{Water}_{Pump}	work of the water pump (kW)
W^{EtOL}_{Pump}	work of the ethanol pump (kW)

Greek letters

η_C	cooling system efficiency
η_{FCS}	fuel cell system efficiency
η_{FP}	fuel processor efficiency
φ	overpotential (V)

Subscripts

a	anode
c	cathode

Superscripts

in	input
out	output
HHV	higher heating value
LHV	lower heating value

order to analyze the sensitivity of the main decision parameters and to determine the major integration bottlenecks. This step also aims at understanding the influence of constraints and evaluating their importance on the system performance. The system includes an ethanol steam reforming (ESR), water gas shift (WGS) and preferential oxidation (PrOx) reactors for the fuel processing, followed by a proton exchange membrane cell stack (PEMFC) and a post-combustion unit. It is intended to study the influence of the following operating variables and configurations on the integrated system efficiency: operating conditions of the reformer, effect of the inlet temperature to the WGS and PrOx reactors, combustion preheating, expander unit, and crude ethanol as fuel.

Few works have addressed the thermodynamic analysis of ethanol processors [13–15]. Ioannides [13] analyzed the ethanol steam reforming but without considering process integration. Song et al. [14] investigated an integrated ethanol fuelled proton exchange membrane fuel cell by exergy analysis. Örücü et al. [15] considered the catalytic conversion of ethanol to hydrogen by indirect partial oxidation. Lyubovsky and Walsh [7] described a fuel processor based on methanol autothermal reforming reactor operating at high pressures followed by membrane-based hydrogen separation.

Process simulation software has been widely used for evaluating fuel cell systems performance [16–18]. In this work, a commercial simulator was used to solve the mass and energy balances, and to compute the operating conditions for the process units. The process under study was implemented within HYSYS flow sheeting software [19]. Maximum heat integration within the system is necessary to achieve acceptable net electrical efficiency levels. The use of process integration techniques applying pinch analysis has already been reported for the design of a heat exchange network for integrated PEM fuel cell systems [10,11,20]. In this paper, the heat exchanger network involving the reformer, burner, gas cleaning units and the PEMFC stack was modeled using the LNG exchanger model within HYSYS. This allows identifying the most successful heat exchange opportunities, and to define the optimal operating conditions of the ethanol processor for obtaining the best overall efficiency considering the plant balance. The analysis here considered will serve as a basis for further process design including the optimal structure determination.

2. Description of the ethanol processor

The fuel cell system includes a fuel processor, which chemically converts ethanol to hydrogen, a hydrogen cleanup equipment, a fuel cell stack, which electrochemically converts the hydrogen energy to electric power, associated equipment for heat, air and water management, and auxiliary equipment such as pumps and blowers.

The fuel processing process has been built according to Little [12]. Fig. 1 shows the main components: ethanol steam reformer (ESR), high (HTS) and low (LTS) temperature water gas shift reactors, a preferential oxidation reactor of CO (PrOx), a proton exchange membrane fuel cell (PEMFC), a combustor, compressors and an expander.

As this simulation case was developed for system design, the pressure drops are neglected and the operating pressure is fixed at 3 atm.

The inlet flows depicted in Fig. 1 are the following: Stream #01 is the ethanol flow provided at 25 °C. Stream #02 is the water flow required for the steam reformer whose flow rate is controlled by the water to ethanol molar ratio. Stream #30 is the airflow required for the operation of combustor, fuel cell and the PrOx unit. In the integrated system, the air compressor will be driven by a turbine expanding the post combustion gases.

The compressor, expander and pumps isentropic efficiencies are 75%. The inlet air conditions are 1 atm, 25 °C.

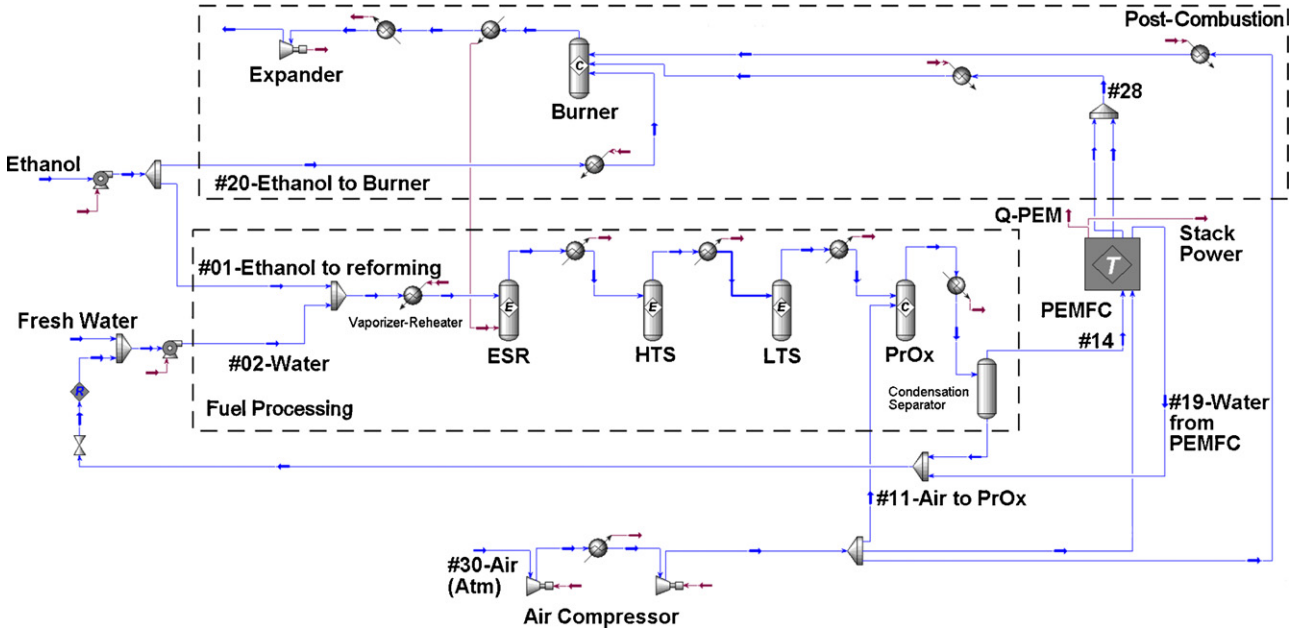

Fig. 1. Fuel cell system components and their heat exchange needs.

2.1. Ethanol steam reforming

In order to generate a hydrogen-rich stream from a fuel processor, ethanol is converted in a reforming unit that involves steam reforming (feed is composed of fuel and steam). Thermodynamic studies [21–23] have shown that the steam reforming of ethanol is feasible being methane, carbon oxides and hydrogen the main products. The steam reforming of alcohols for hydrogen production involves a complex multiple reaction system, the purity of a hydrogen product is affected by many undesirable side reactions [2,3]. Therefore, hydrogen yield is closely related to the process variables such as pressure, temperature, reactants ratio, and on the catalyst being used.

In the present study two possible pathways are considered. The first analyzed route (case A) considers that the reformer performs the following reactions according to the mechanism proposed by Benito et al. [4] for a Co/ZrO_2 catalyst:

Ethanol dehydrogenation

$$C_2H_5OH \rightarrow CH_3CHO + H_2, \quad \Delta H^\circ_{298} = 71\,kJ/mol \tag{1}$$

Acetaldehyde decomposition

$$CH_3CHO \rightarrow CH_4 + CO, \quad \Delta H^\circ_{298} = -21.9\,kJ/mol \tag{2}$$

Methane steam reforming

$$CH_4 + H_2O \leftrightarrow CO + 3H_2, \quad \Delta H^\circ_{298} = 206.14\,kJ/mol \tag{3}$$

Water gas shift (WGS):

$$CO + H_2O \leftrightarrow CO_2 + H_2, \quad \Delta H^\circ_{298} = -4.1\,kJ/mol \tag{4}$$

To achieve a good yield following this reaction scheme, it is necessary to operate at high temperature (>550 °C) in order to favor the methane steam reforming reaction.

A second proposal (case B) considers the equilibrium composition of the water gas shift reaction (4) and the endothermic ethanol decomposition reaction:

$$C_2H_5OH + 3H_2O \leftrightarrow 2CO_2 + 3H_2, \quad \Delta H^\circ_{298} = 170.41\,kJ/mol \tag{5}$$

This pathway is an ideal case where no intermediate compounds are formed. This scheme was previously analyzed by Song et al. [14]. In both cases, all reactions are supposed to be at equilibrium.

The reactor is supposed to be isothermal, meaning that heat has to be supplied to maintain the temperature in the reactor from an external energy source. In conventional tubular steam reforming, the energy to drive the endothermic reforming reactions is supplied by external heating through the tube wall, generally through combustion of a portion of the fuel. In this study, the reforming temperature (T_{Ref}) and the water to ethanol molar ratio (R) have been considered as being the major decision variables for the analysis.

The thermodynamic behavior of both pathways is different. In a reformer unit the hydrogen yield depends on the water-to-ethanol molar ratio, temperature and pressure. In Case A, H_2 production is favored by higher molar ratios and higher temperatures. At $R = 20$ and $T_{Ref} = 900\,^\circ C$, 5.48 mol of H_2 per mol of ethanol fed to the reformer is produced. The presence of methane as intermediate requires higher temperatures to achieve a better yield.

For the other case, the maximum yield occurs at lower temperatures. At $R = 20$ and $T_{Ref} = 300\,^\circ C$, it is produced 5.98 mol of H_2 per mol of ethanol. These values obtained by thermodynamic analysis correspond to a pressure of 3 atm. In both cases higher water-to-ethanol ratios resulted in better yields. However, optimal operating conditions will be determined by a global efficiency analysis.

2.2. Water gas shift reactors

CO produced from reforming reactions must be brought down to ppm levels because it gets adsorbed on the noble catalyst of the PEMFC and poisons it. This task is partially accomplished by water gas shift reactors. These units proceed with the exothermal WGS reaction that is supposed to be at equilibrium. This step also leads to additional H_2 generation. The water gas shift reaction is usually carried out in two adiabatic shift reactors in series with an inter-cooler in between to remove the heat of reaction of the exothermic water gas shift reaction. The fist-stage reactor typically operates at 350–500 °C and is called the high-temperature shift (HTS) reactor. The HTS reactor uses a chromiun-promoted iron oxide catalyst. The second stage is a low-temperature shift (LTS) reactor, which operates at 150–250 °C, using a copper–zinc catalyst supported on alumina. The LTS is capable of achieving a residual CO concentration in the order of 0.5–1.5 dry vol.%.

Performance of these units depends on input concentration of CO and H_2O/CO ratio. Such variables are related to R, T_{Ref} and the reformer reaction pathway. Besides, input temperatures affect performance because they modify the output temperature varying the CO conversion.

2.3. Preferential oxidation reactor

Chemical equilibrium limits the conversion achieved in the WGS reactor, thus, final CO cleanup occurs in a preferential oxidation (PrOx) unit in which the desired reaction is the oxidation of carbon monoxide. This reactor is required to reach a very low level of CO content in the fuel stream at the fuel cell inlet in order to avoid fuel cell catalyst poisoning. It uses oxygen to proceed with the following reaction:

$$CO + \tfrac{1}{2}O_2 \rightarrow CO_2.$$

Unfortunately, the selectivity of the catalyst will not avoid the combustion of some hydrogen in the gas stream with the following reaction:

$$H_2 + \tfrac{1}{2}O_2 \rightarrow H_2O.$$

The airflow rate (stream #11) is computed as a function of the CO flow rate assuming two moles of O_2 per mole of CO. In the model, the CO oxidation is completed until it achieves 10 ppm at the reactor outlet. The remaining O_2 reacts totally with hydrogen, which represents a selectivity (mol H_2 consumed per mol CO consumed) of about 3. An adiabatic operation has been considered for the PrOx reactor. Performance of this reactor depends on the CO inlet concentration that is related to R and T_{Ref} in the steam reformer.

2.4. Proton exchange membrane fuel cell stack model

The fuel cell stack model is equilibrium based and adopted from Godat and Marechal [10]. The ideal unit cell voltage is computed as follows:

$$E_{Rev} = E^0_{Rev}(T_{Cell}) + \frac{R_g T_{Cell}}{2F}\left[\ln(p^*_{H_2,a}) + \frac{1}{2}\ln(p^*_{O_2,c})\right] \quad (6)$$

Here, E_{Rev} is the cell voltage adjusted to the cell temperature (T_{Cell}), $p^*_{H_2,a}$ and $p^*_{O_2,c}$ are the partial pressures of the H_2 and O_2 averaged (arithmetic mean) between the inlet and outlet conditions.

Useful work (electrical energy) is obtained from a fuel cell only when a current is drawn, but the actual cell voltage (V_{Cell}) is decreased from its equilibrium thermodynamic potential (E_{Rev}) because of irreversible losses. When current flows, a deviation from the thermodynamic potential occurs corresponding to the electrical work performed by the cell. Therefore, the expression of the voltage of a single cell is $V_{Cell} = E_{Rev} - \varphi$, where φ is the drop potential due to irreversibilities of the operation, which represents the deviation from the equilibrium value.

The actual electrical power generated by the cell (P_{Cell}) can then be calculated from $P_{Cell} = V_{Cell} l_{Cell}$. We defined the operating voltage as the power level at which unit cell voltage drops to 0.5 V from the ideal voltage [20].

The current l_{Cell} is related with the hydrogen molar flow rate at the anode.

$$l_{Cell} = 2F(f^{in}_{H_2,a} - f^{out}_{H_2,a}) \quad (7)$$

The fuel utilization is considered to be 80%. The PEM is supposed to be isothermal and isobar. We considered a system pressure of 3 atm and fuel cell temperature of 80 °C. The inlet oxidant to the cathode is humidified to a relative humidity of 80% and the anode inlet stream is always fed at saturated condition. Oxygen stoichiometry is two in the calculations representing an oxidant utilization of 50%.

In order to compute the PEM fuel cell cooling, an energy balance is made over the cell from the inlet to the exit conditions. The heat produced by the cell and necessary to dissipate then becomes,

$$Q_{PEM} = \sum_{i=1}^{inlets} f_i h_i(T_{Cell}) - \sum_{o=1}^{outlets} f_0 h_0(T_{Cell}) - P_{Cell} \quad (8)$$

2.5. Post-combustion system

The depleted fuel of the PEMFC, formed by cathode and anode outlets, is burnt off in the post combustion system. The generated heat will be used to balance the energy requirement of the fuel processing section. Supplementary firing of ethanol (stream #20) will be considered if the energy content of the depleted fuel is not sufficient to satisfy the balance. The supplementary fuel requirement will be computed in order to achieve a set of feasibility specifications. A minimum approach temperature of $\Delta T = 100$ °C in the cold side of the reformer is first imposed. Complete and stoichiometric combustion for the burner unit has been assumed.

After the heat exchange with the LNG unit, the exhaust gases can be expanded in a turbine coupled to the air compressor.

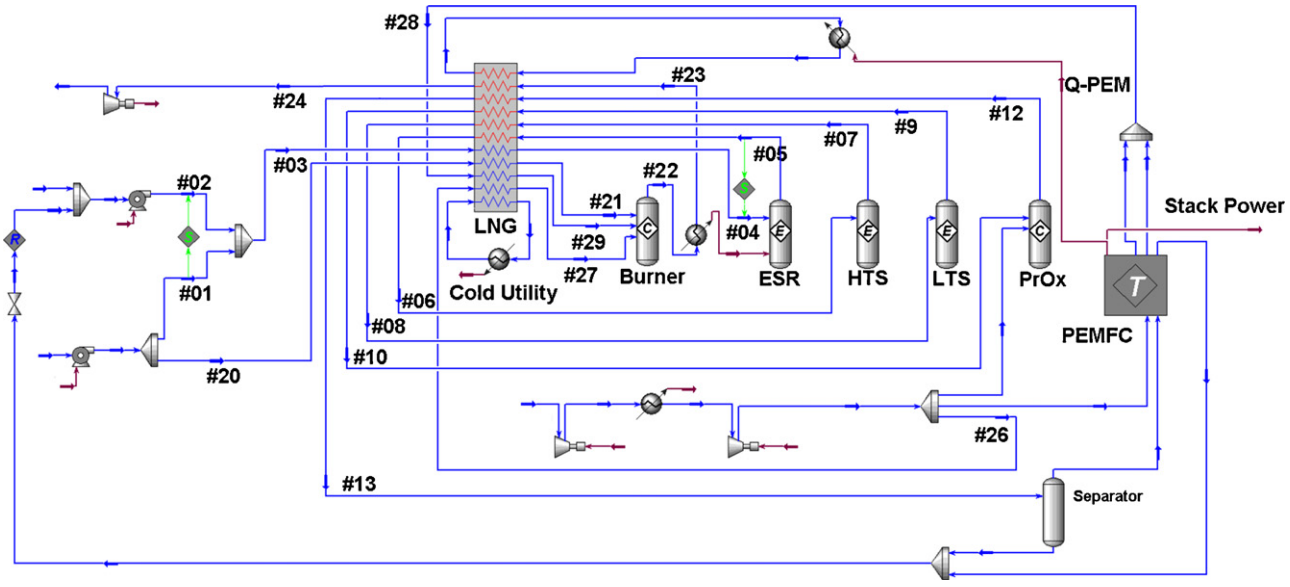

Fig. 2. Integrated system.

Additional ethanol burning will be considered, if necessary, to balance the air compression work requirement.

2.6. Heat exchange model

The heat exchangers have been considered in the simulation model described above resorting to the LNG unit of HYSYS (Fig. 2).

The LNG exchanger model is a HYSYS operation that solves heat and material balances for multi-stream heat exchangers and heat exchanger networks. The LNG calculations are based on energy balances for the hot and cold fluids. Each stream is divided using 20 intervals, and phase change is verified. In this approach, the results of the simulation model will characterize the hot and cold streams of the system. Table 1 summarized the thermal requirement for the fuel processor streams connected to the LNG unit.

The LNG unit allows analyzing the system energy integration by means of the process integration method (or pinch technology) [24]. Process integration studies start with the definition of a list of hot and cold streams. The hot and cold streams define, respectively, heat sources and heat requirements of the system that are characterized by a heat–temperature diagram usually specified by a heat load, an inlet and a target temperature. The heat sources are then composed to compute the hot composite curve that represents the heat availability in the system as a function of the temperature. The same procedure is applied for the cold streams to draw the cold composite curve. Considering that the heat exchange will be technically feasible if the temperature difference between the hot and cold streams will always be superior to a predefined $\Delta T_{\min}$, the maximum heat recovery by heat exchange between the hot and the cold streams will be obtained when the $\Delta T_{\min}$ constraint is activated. This point is called the system pinch point. By means of energy balance, one may then compute the minimum energy requirement of the system and the minimum heat to be evacuated from the system. Using the composite curve calculation together with a simulation model, we define the simulation of the heat exchangers network without knowing about its configuration. With this approach, we will be able to compute the influence of the decision variables so that the best system configuration can be then defined.

Table 1
Fuel processor streams connected to the LNG unit

No.	Type	Description	T_{in} (°C)	T_{out} (°C)
1	Cold	Water/ethanol mixture heating for the SER reaction	T_{Mix}	T_{Ref}
2	Cold	Anode and cathode gases from FC, preheating for the combustion	80	500
3	Cold	Extra ethanol preheating for the combustion	25	300
4	Cold	Air preheating for the combustion	$T^{\text{out}}_{\text{Comp}}$	300
5	Cold	Cold utility	20	25
6	Hot	Stream between the SER and HTS	T_{Ref}	500
7	Hot	Stream between the HTS and LTS	$T^{\text{out}}_{\text{HTS}}$	150
8	Hot	Stream between the LTS and PrOx	$T^{\text{out}}_{\text{LTS}}$	237
9	Hot	Stream between the PrOx and the PEM inlet	$T^{\text{out}}_{\text{PrOx}}$	80
10	Hot	Combustion gases after ESR to gas turbine	T_{cg}	$T^{\text{in}}_{\text{Tur}}$
11	Hot	PEMFC heat remove	65	55

2.7. Definition of efficiencies

The overall efficiency of the FCS is defined here as the net energy output of the system obtained from the gross output by subtracting the electrical energy needed to operate FCS auxiliaries such as pumps and compressors divided by the heating value of the ethanol consumed in the fuel processor for reforming (f_{EtOL}^{FP}) and burning (f_{EtOL}^{Bum}).

$$\eta_{FCS}^{HV} = \frac{P_{System}}{(HV_{EtOL}(f_{EtOL}^{FP} + f_{EtOL}^{Bum}))} \quad (9)$$

The HV factor can be the higher heating value (HHV) or the lower heating value (LHV) of the ethanol. HHV represents the actual amount of chemical energy in the fuel (relative to standard conditions), while LHV neglects heat below 150 °C. Therefore, HHV should be compared with the mechanical and electrical energy produced by the power system [25]. However, as LHV value is used in numerous works is useful to report both values.

The net power of the system is computed as follows:

$$P_{System} = P_{cell} - W_{Pump}^{Water} - W_{Pump}^{EtOL} - \frac{Q_{Cooler}}{\eta_c} - (P_{Comp} - P_{Tur}) \quad (10)$$

where W_{Pump}^{Water} and W_{Pump}^{EtOL} are the work of the water and ethanol pumps, respectively. Q_{Cooler} is the heat removal from the fuel cell system; it represents the cold utility of the process. This heat is formed by the heat generated by the fuel cell and extra cold utilities such as heat removal from PrOx outlet stream in the condenser separation unit in order to meet the fuel cell operating temperature. In the above expression, η_c is the cooling system efficiency defined as the rate of heat removal over the electrical power consumed by the pumps and fans associated to the refrigeration system [26]. We considered a cooling system efficiency of 25%.

The processor efficiency is defined as the ratio of the heating value of the gas stream incoming to the anode (stream #14) divided by the sum of the heating value of the ethanol fed to the processor (stream #02 and #20) and the tail gas purged from the stack (stream #28). Again, the processor efficiency can be computed based on the lower or higher heating values.

3. Results and discussions

The integrated process model has been used to determine the optimal operating conditions to be considered in the system. The influence of the water-to-ethanol molar ratio and reforming temperature has been studied. Furthermore, the remaining reactors temperatures were considered as variables, but the changes in efficiency due to these variables are marginal.

As previously mentioned in Section 2.5 the procedure of calculation to close the energy balance is the following: fixing the water-to-ethanol molar ratio and the reforming temperature, the simulation model determines the temperature of combustion gases (T_{cg}) which leave the reformer unit (stream #23). If this temperature is lower than $T_{Ref} + \Delta T$, an extra amount of ethanol is burned (steam #20), which is computed in order to achieve this thermal requirement ($\Delta T = 100$ °C). Flue gases will exchange heat with the other units, by means of the LNG operation, before being expanded in a turbine. If the flue gases temperature, after this heat exchange, is lower than the inlet temperature in the turbine (T_{Tur}^{in}) necessary to balance the air compression work, a supplementary burning of ethanol is computed.

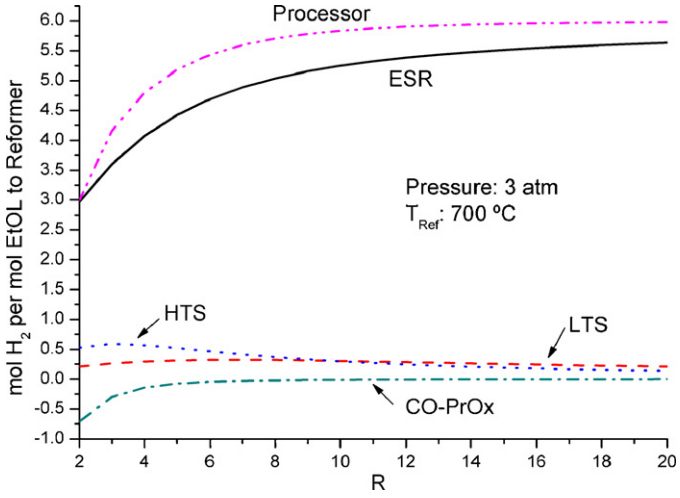

Fig. 3. Reactors yields vs. water-to-ethanol molar ratio.

The next subsections present results obtained considering the reaction pathway A for the reformer. The input temperature has been fixed at 500 °C, 150 °C and 237 °C for the first WGS reactor, the second WGS reactor and the PrOx reactor, respectively [12]. In Section 3.3, a comparative analysis between reaction pathways A and B is considered.

3.1. Influence of the water-to-ethanol ratio

In this section, the effect of the water-to-ethanol ratio on the net efficiency of the system will be analyzed. The Fig. 3 presents the reactors yields and the total yield of the processor. These yields are computed as the ratio of mol of hydrogen produced by mol of ethanol incoming to the reformer.

Although a high reagents molar relation presents a good yield of hydrogen, the water quantity demands extra energy in the vaporization and reheating processes before entering to the reformer. This extra energy is partially recovered from the hot streams, which increase their flow rate, but heat exchanges occur at finite temperature differences and consequently efficiency decreases. Fig. 4 shows global efficiency and energy demand of the evaporator, reheater and reforming reactor versus the water-to-ethanol molar ratio at constant reforming temperature ($T_{Ref} = 700$ °C).

Smaller molar ratios present lower efficiency because reformer yield is lower. Besides the CO produced is increased and the PrOx unit consumes more H_2 to reduce the level of CO to the required values. At higher water-to-ethanol molar ratios, the water excess must be evaporated and re-heated consuming additional fuel in the reformer, diminishing then the system efficiency. Due to water excess, thermodynamic equilibrium of the water–gas-shift reaction on both HTS and LTS reactors is shift

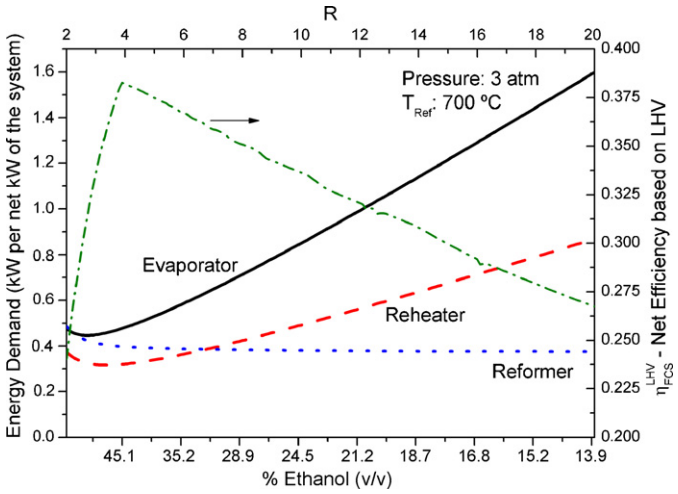

Fig. 4. Efficiency and energy demand vs. the water-to-ethanol molar ratio.

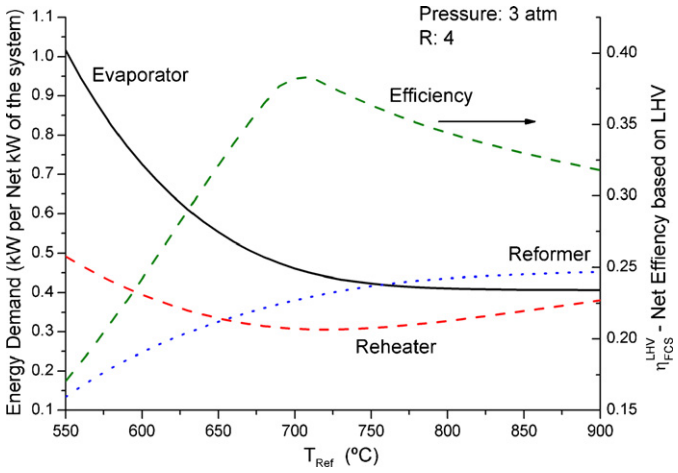

Fig. 6. Efficiency and energy demand vs. reforming temperature.

to hydrogen formation diminishing the CO outlet concentration. This improves the performance of PrOx reactor, consuming less H_2 at higher R values.

3.2. Influence of reformer temperature

The effect of the reforming temperature is analyzed considering the water-to-ethanol molar ratio of 4. The yield of the reactors (Fig. 5) show that increasing the temperature the hydrogen production increases in the reformer, HTS and LTS units, although the hydrogen consumed by the PrOx unit is increased too.

Fig. 6 shows the variation of the energy demand with the temperature. The demand of the evaporator decreases, the reactor increases and the reheater presents a minimum.

Operating at lower temperatures, the poor yield of hydrogen implies a greater flow of reactive mixture needed to achieve the target power. This superior flow increases the energy demand of the evaporator.

The energy demand of the reformer increases because the conversion of methane is enhanced with the temperature, producing greater energy requirements.

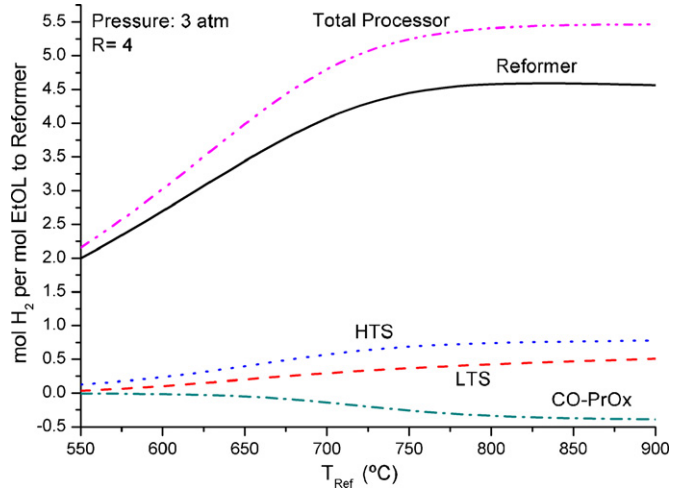

Fig. 5. Reactors yield vs. reforming temperature.

The sum of these effects produces a maximum net efficiency of $\eta_{FCS}^{LHV} = 38\%$ below 709 °C.

3.3. Effect of the pathway of the reactions

In Figs. 7 and 8, a 3D surface is presented where the global efficiency of the system based on LHV is shown. We present efficiency as a function of the water-to-ethanol molar ratio and reforming temperature. Fig. 8 has the axes interchanged to clarify the view of the surface.

Fig. 7 represents results for the reactions scheme A, maximum efficiency of $\eta_{FCS}^{LHV} = 38\%$ occur at $T_{Ref} = 709\,^{\circ}C$ and $R = 4$, and the fuel processor efficiency is $\eta_{FP}^{LHV} = 80.5\%$. Efficiencies based on higher heating value are $\eta_{FCS}^{HHV} = 35\%$ and $\eta_{FP}^{HHV} = 80.6\%$.

For the reaction pathway Case B (Fig. 8), maximum efficiencies are $\eta_{FCS}^{LHV} = 39\%$ and $\eta_{FCS}^{HHV} = 36\%$ at $T_{Ref} = 308\,^{\circ}C$

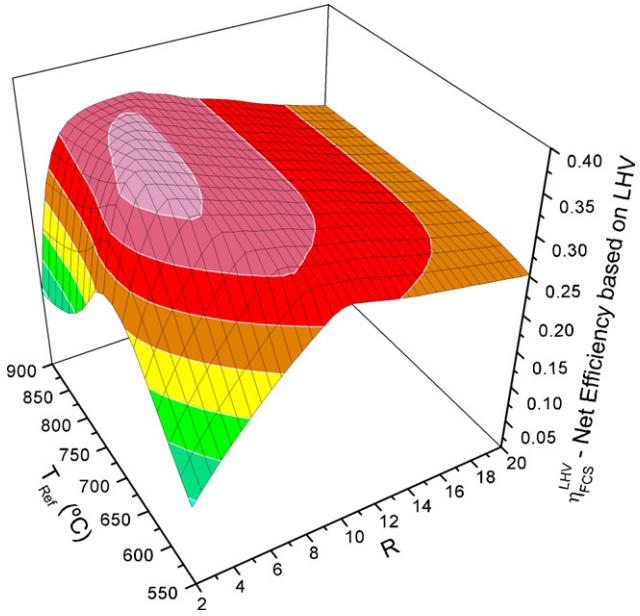

Fig. 7. Net system efficiency. Pathway A.

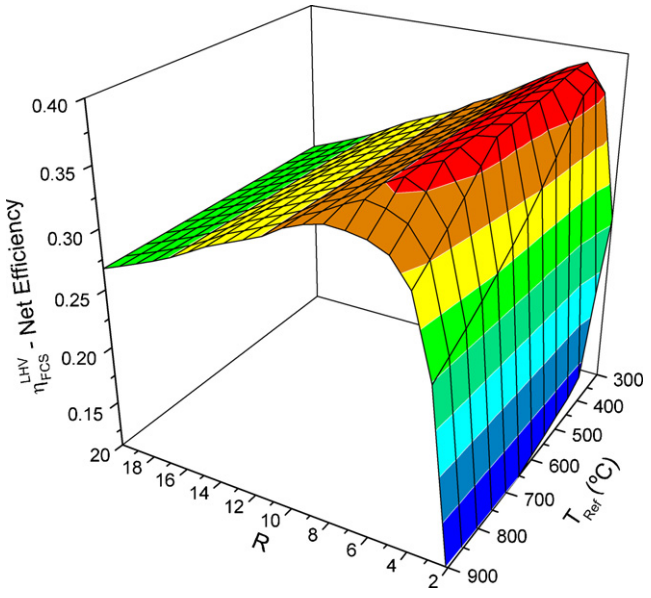

Fig. 8. Net system efficiency. Pathway B.

and $R = 3.2$ and the processor efficiencies are $\eta_{FP}^{LHV} = 81.4\%$ and $\eta_{FP}^{HHV} = 80.6\%$. This suggests that the effect of the catalyst employed in the ethanol steam reforming will not affect the net efficiency of the system, but operating conditions could vary drastically.

From the figure, we can conclude that there is a region where efficiencies vary insignificantly. This suggests that working at $R = 4$ or 5 do not affect the net efficiency in a major grade. This is consistent with practical use, where a water excess respect to the stoichiometric values additionally prevents coke formation and deposition onto the catalyst.

The optimal water-to-ethanol molar ratio and temperature considering the reformer alone, does not agree with the operation point calculated from a global efficiency analysis (Fig. 7). This fact indicates the importance of optimizing an integrated system rather than optimizing process units separately.

3.4. The self-sufficient limit

The self-sufficient limit of the system is the limit at which the un-reacted hydrogen that leaves the anode and other fuels present at the outlet of the fuel cell as CH_4, allows satisfying the energy requirement of the system. In the Fig. 9 the self-sufficient limit divides the operating conditions in two zones. In the zone above this limit (black line), the depleted fuel satisfies the energy requirement of the system, even though the overall efficiency is lower than the cases where an extra fuel is necessary to feed the combustor. The white line indicates the temperature that presents maximum net efficiency for each value of R. Both lines are coincident in a brief stretch.

3.5. Composite curves

In the late 70s Pinch technology emerged as a tool for the design of heat exchanger networks [24]. One of the most significant features of pinch analysis is that it can be used to set performance targets for a process before a detailed design. Most importantly, these design options are evaluated in a whole-process context to ensure that they give a global improvement. Once a process configuration and conditions that give satisfactory targets have been established, then a heat exchanger network (HEN) is designed. The pinch design method makes this design task relatively simple.

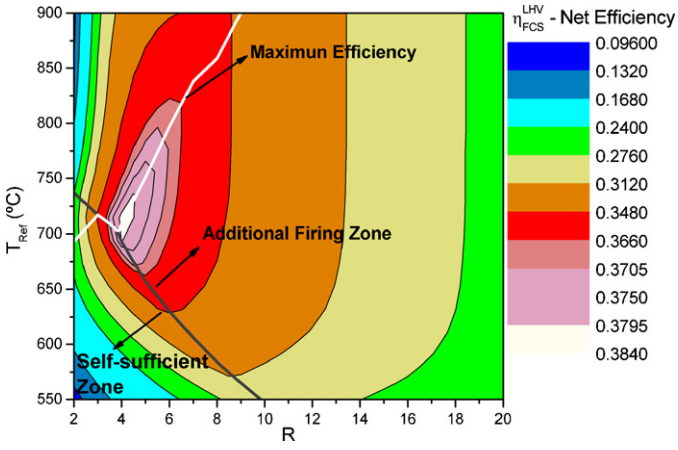

Fig. 9. The self-sufficient limit.

The system composite curves were drawn in order to give a good view of the possibilities for a heat exchanger network (Fig. 10). The composite curves are two curves describing the total system cooling and heating demand, respectively, as a function of temperature intervals. Using the LNG operation we can build the composite curves from the system. Fig. 10 shows the composite curves of the system for the optimal operating conditions of case A. Table 2 shows the input and output process stream compositions of main process units (reactors and fuel cell) obtained at these operating conditions.

For the LNG operation, heating and cooling demand between reactors was calculated: all internal streams were forced to their working temperatures, and all heating or cooling demands for all streams were recorded (Table 3). Note that every single inlet

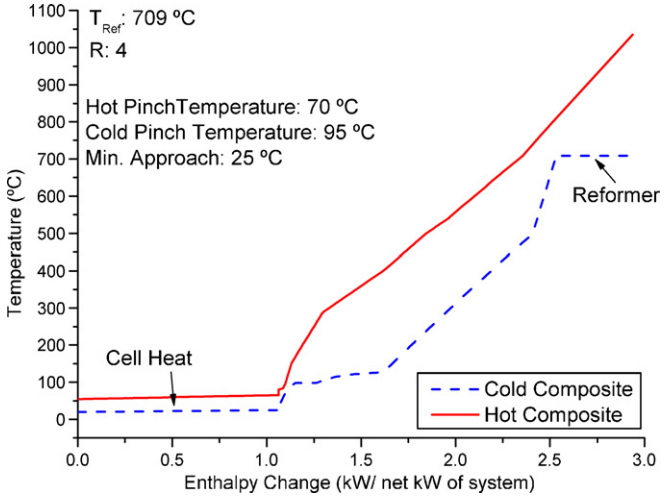

Fig. 10. Composite curves for optimal $T_{Ref} = 709$, $R = 4$.

Table 2
Input and output data of main units

Stream number	#04	#05	#07	#09	#12	#14	#28
Temperature (°C)	709	709	539	237	406	80	80
Pressure (atm)	3	3	3	3	3	3	3
Mole flow (kmol h^{-1})	0.0367	0.0628	0.0628	0.0628	0.0658	0.0636	0.1749
Molar fraction							
Hydrogen	0.0000	0.4860	0.5221	0.5921	0.5475	0.5666	0.0412
H_2O	0.8000	0.2804	0.2443	0.1743	0.1844	0.1559	0.1559
Methane	0.0000	0.0256	0.0256	0.0256	0.0245	0.0253	0.0092
CO	0.0000	0.1123	0.0763	0.0063	0.0000	0.0000	0.0000
CO_2	0.0000	0.0957	0.1317	0.2017	0.1986	0.2056	0.0747
Ethanol	0.2000	0.0000	0.0000	0.0000	0.0000	0.0000	0.0000
Oxygen	0.0000	0.0000	0.0000	0.0000	0.0000	0.0000	0.0824
Nitrogen	0.0000	0.0000	0.0000	0.0000	0.0450	0.0466	0.6366

stream to the fuel cell system was preheated to its working temperature and also included.

The net electric efficiency based on HHV is approximately 35%. The remaining 65% is accounted for: dissipation as heat in the PEMFC cooling system (38%), energy in the flue gases (10%) and irreversibility in compression and expansion of gases. The tasks that demand more energy are vaporizing and reheating of the reactive mixture (0.79 kW), the reformer reactor (0.41 kW) and the preheating of the exhaust gas to the burner (0.67 kW). These values represent the energy demand – in kW – per net kW produced by the system. Pass #28 to #29 requirement is comparatively high due to the more significant flow rate of this stream because of the presence of N_2.

Of the needed energy to drive the FCS auxiliaries, mainly pumps and blowers for water, ethanol, air and heat management, the largest load is the air compressor (0.16 kW), which delivers air to the cathode compartments of the stack and to the PrOx reactor.

Fig. 11 compares the composite curves for two different water-to-ethanol molar ratios. It shows the previously analyzed case, corresponding to $R = 4$ (maximum efficiency case), and for $R = 10$ at the same operating reforming temperature. As can we see in Table 3, the extra water quantity increases an 80% the energy demand in the evaporator, and a 33% the cold utility. These changes move the composite curves producing a net efficiency based on HHV of 31%.

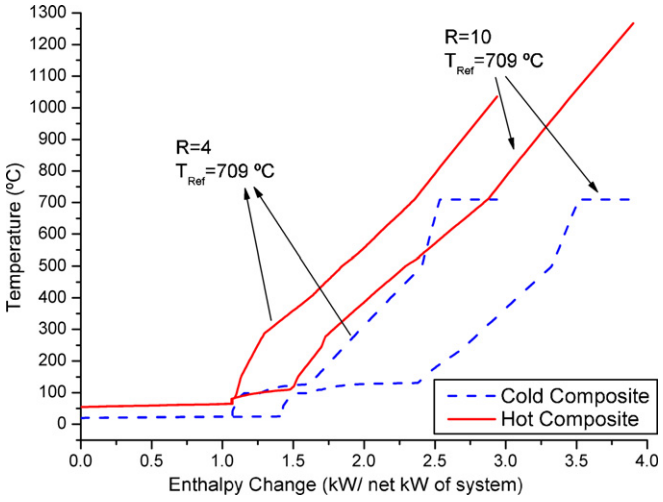

Fig. 11. Comparative composite curves for $R = 4$ and $R = 10$.

Table 3
Heating and cooling demands for the system streams

Pass		$R = 4$			$R = 10$		
		Input (°C)	Output (°C)	Q (kW)	Input (°C)	Output (°C)	Q (kW)
#03–#04 (vaporizing)	Cold	42	126	0.47	59	131	0.85
#03–#04 (reheater)	Cold	127	709	0.32	131	709	0.50
#28–#29	Cold	80	500	0.67	80	500	0.65
#20–#21	Cold	25	300	0.01	25	300	0.05
#26–#27	Cold	116	300	0.00	116	300	0.00
Cold utility	Cold	20	25	1.07	20	25	1.43
ESR duty	Cold	709	709	0.41	709	709	0.38
#05–#06	Hot	709	500	0.13	709	500	0.20
#07–#08	Hot	539	150	0.23	522	150	0.34
#09–#10	Hot	237	237	0.00	174	237	0.06
#12–#13	Hot	406	80	0.23	244	80	0.51
#23–#24	Hot	811	287	0.88	1065	278	1.37
#22–#23	Hot	1035	810	0.41	1267	1065	0.38
Q-PEM	Hot	65	55	1.06	65	55	1.07

Table 4
Effect of input temperatures of the clean-up system reactors

η_{FCS}^{LHV} (%)	η_{FCS}^{HHV} (%)	HTS (°C)	LTS (°C)	PrOx (°C)	T_{Ref} (°C)	R molar
38.3	34.9	500	150	237	709	4.0
38.3	34.9	500	150	150	704	3.8
38.8	35.3	350	150	237	709	3.6
38.8	35.3	350	150	150	709	3.6
39.3	35.8	150	150	150	714	3.3

3.6. Effect of input temperatures of the clean-up system reactors

In previous analyses, input temperatures to HTS, LTS and PrOx reactors were fixed following the scheme proposed by Little [12]. HTS and LTS units are modeled as equilibrium reactors and in the PrOx the conversion is fixed. These units operate at adiabatic conditions, so input temperature variation modifies the output temperature. In addition, the CO conversion in the WGS units is modified.

Table 4 shows the new values of operating reformer variables that maximize the efficiency when the input temperatures of the train of purification reactors are varied.

Some conditions of the temperature selected could be outside the reasonable operating parameters and may change the structure of the processor; i.e. two stages of WG reactors operating at 150 °C imply two reactors of LTS. Besides, PrOx operating temperature variation could vary the selectivity to burning hydrogen (which is not accounted for in the model). However, the goal is to analyze the sensitivity of the net system efficiency on the input temperature without considering design aspects of each reactor.

In the table, T_{Ref} and R represent the new optimal conditions calculated for each case.

The variation of the input temperatures does not affect sensitively the net efficiency of the system even though the operating conditions of the reformer are modified. The net efficiency differs slightly. However, smaller molar optimal relations are found when input reactor temperatures decrease.

3.7. Influence of the combustion preheating

The burner is fed with three streams: pure ethanol, air and depleted gases from PEMFC. In the cases under study, the oxygen from de cathode exhaust is enough to burn the fuel (H_2, CH_4, EtOL) in stoichiometric form. Consequently, there is no need of extra air. These streams are previously heated (combustion preheating) allowing a heat recover from below the reforming temperature to make it available above the reforming temperature.

In Table 5 efficiency values for several preheated temperatures of gases to burn are shown. The results reveal that by increasing the input temperature of the burner the required amount of additional fuel is reduced. Efficiency based on HHV is about 35% with preheating while it is 28% without preheating.

Table 5
Influence of the combustion preheating

T (°C)	η_{FCS}^{LHV} (%)	η_{FCS}^{HHV} (%)	Ethanol to burn (mol h^{-1})
80	30.4	27.7	2.15
200	32.3	29.4	1.62
300	34.0	31.0	1.17
400	36.1	32.8	0.71
500	38.3	34.9	0.25
600	38.3	34.9	0.25
700	38.3	34.9	0.25

3.8. Crude ethanol as reforming fuel

The fermentation broth produced from a fermentation process contains approximately 12% (v/v) ethanol and other oxygenated hydrocarbons, called crude ethanol [6]. In this section, this blend is considered as feed to the processor. However, the fuel feeding the burner was considered pure ethanol due to the lower heating value of the crude ethanol.

The main advantage of this feedstock is to eliminate the large amount of energy wasted during distillation to remove water from fermentation broth in order to produce dry or pure ethanol.

The water-to-ethanol molar ratio for this mixture is $R = 20$. In Fig. 12, the effect of the reforming temperature on the net efficiency of the system is shown. Because of the high water content, more energy is necessary in the vaporizer and reheat steps, decreasing the maximum net efficiency to levels of $\eta_{FCS}^{LHV} = 27\%$ and $\eta_{FCS}^{HHV} = 24\%$. These levels are lower than those previously

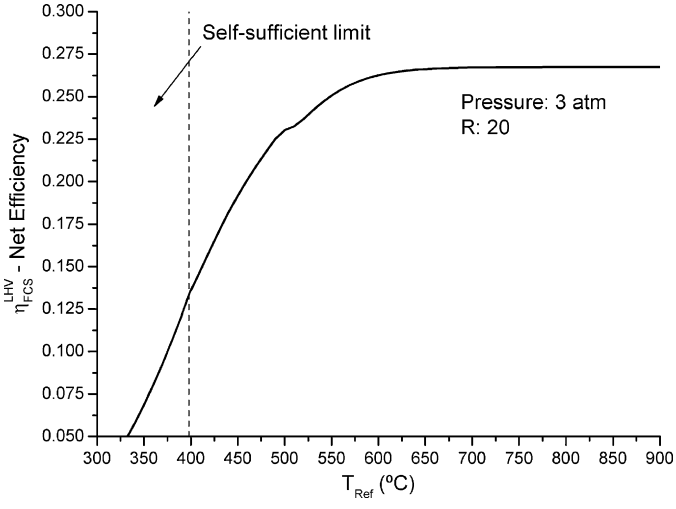

Fig. 12. Crude ethanol fuelling the reformer reactor.

Table 6
Influence of the turbine on the net efficiency of the system

	η_{FCS}^{LHV} (%)	η_{FCS}^{HHV} (%)	R	T_{Ref} (°C)	P_{Comp} (kW)	P_{Tur} (kW)	Power stack (kW)	Net power (kW)
$P_{Tur} = 0$	34.4	31.3	5.5	679	0.17	–	1.24	1
$P_{Tur} = P_{Comp}$	38.3	34.9	4.0	709	0.16	0.16	1.04	1
$P_{Tur} \leq P_{Comp}$	38.9	35.3	4.9	687	0.16	0.13	1.08	1

examined, but using crude ethanol allows circumventing the distillation and drying steps. The energy saving of these steps is not being considered in the present study. The ethanol processor can be integrated with any existing ethanol production plant by placing it after the fermentation step but before the distillation and drying stages.

3.9. Efficiency analysis without considered expander unit

In the previous sections the fuel cell system was analyzed considering that the required compression work was balanced with a turbine. The goal here is to study the effect on the net efficiency when the expander unit is not present. Table 6 presents the results obtained considering the following cases: without turbine; work turbine matches the compression work; partial work recuperation with the turbine. The second case was utilized in all previous analyses considering extra ethanol burning to balance both works. The last case considers that the turbine is present, but when compression work is superior to the expander unit, the difference is balanced by means of the fuel cell power.

This analysis shows that the best option is working with a partial recovery of work. Net efficiency is slightly improved when it is compared with total recovery, but the operating conditions vary significantly.

4. Conclusions

A simulation model of a fuel cell system fuelled by ethanol has been built-up to analyze the process performance for stationary or mobile applications. The heat exchanger network was implemented using the LNG HYSYS unit, which allows analyzing the system energy integration by the process integration method. This approach proves to be very interesting in order to study the impact of the major decisions parameters (water-to-ethanol molar ratio, reforming temperature).

Total system efficiencies up to 35% based on HHV were computed considering methane as intermediate in the reformer unit. When not considering the methane like intermediary, the efficiency of the system would not be improved, but the operating temperature of the reactor is reduced.

An efficient ethanol processor depends on the operating conditions of the reformer and their efficient energetic integration. The influence of several variables was simulated and discussed showing the capability of the model to evaluate alternative reforming configurations and operating conditions.

This preliminary analysis will be used to design the HEN system and perform a more accurate optimization in order to synthesize the process network.

Acknowledgements

The authors want to acknowledge the financial support from CONICET (Consejo Nacional de Investigaciones Científicas y Técnicas), ANPCYT (Agencia Nacional de Promoción Científica y Técnica) from Argentina.

References

[1] J.R. Mielenz, Curr. Opin. Biotechnol. 4 (2001) 324–329.
[2] A. Haryanto, S. Fernando, N. Murali, S. Adhikari, Energy Fuels 19 (2005) 2098–2106.
[3] P.D. Vaidya, A.E. Rodriguez, Chem. Eng. J. 117 (2006) 39–49.
[4] M. Benito, J.L. Sanz, R. Isabel, R. Padilla, R. Arjona, L. Daza, J. Power Sources 151 (2005) 11–17.
[5] J. Kugai, S. Velu, C. Song, Catal. Lett. 101 (2005) 255–264.
[6] A.J. Akande, R.O. Idem, A.K. Dalai, Appl. Catal. A: Gen. 287 (2005) 159–175.
[7] M. Lyubovsky, D. Walsh, J. Power Sources 162 (2006) 597–605.
[8] G.A. Deluga, J.R. Salge, L.D. Schmidt, X.E. Verykios, Science 303 (2004) 993–997.
[9] J.R. Salge, G.A. Deluga, L.D. Schmidt, J. Catal. 235 (2005) 69–78.
[10] J. Godat, F. Marechal, J. Power Sources 118 (2003) 411–423.
[11] G.M. Ratnamala, N. Shah, V. Mehta, P.V. Rao, S. Devotta, Ind. Eng. Chem. Res. 44 (2005) 1535–1541.
[12] A.D. Little, Multi-Fuel Reformers for Fuel Cells Used in Transportation-Multi-Fuel Reformers. Phase I. Final Report, Report #DOE/CE/50343-2, prepared for U.S. Department of Energy, Office of Transportation Technologies. Arthur D. Little Inc., Cambridge, 1994.
[13] T. Ioannides, J. Power Sources 92 (2001) 17–25.
[14] S. Song, S. Douvartzides, P. Tsiakaras, J. Power Sources 145 (2005) 502–514.
[15] E. Örücü, M. Karakaya, A.K. Avci, Z. Önsan, J. Chem. Technol. Biotechnol. 80 (2005) 1103–1110.
[16] T. Kivisaari, P.C. van der Laag, A. Ramsköld, J. Power Sources 94 (2001) 112–121.
[17] A. Ersoz, H. Olgun, S. Ozdogan, J. Power Sources 154 (2006) 67–73.
[18] A. Ersoz, H. Olgun, S. Ozdogan, Energy 31 (2006) 1490–1500.
[19] HYSYS, AEA Technology. Calgary, Hyprotech Ltd., Canada, 2001.
[20] F. Marechal, F. Palazzi, J. Godat, D. Favrat, Fuel Cells 5 (2005) 5–24.
[21] E.Y. García, M.A. Laborde, Int. J. Hydrogen Energy 16 (1991) 307–312.
[22] K. Vasudeva, N. Mitra, P. Umasankar, S.C. Dhingra, Int. J. Hydrogen Energy 21 (1996) 13–18.
[23] I. Fishtik, A. Alexander, R. Datta, D. Geana, Int. J. Hydrogen Energy 25 (2000) 31–45.
[24] B. Linnhoff, D. Townsend, P. Boland, G.F. Hewitt, B.E.A. Thomas, A.R. Guy, R.H. Marsland, A User Guide on Process Integration for the Efficient Use of Energy, Institute of Chemical Engineers, Rugby, UK, 1985.
[25] Ulf Bossel, Well-to-Wheel Studies, Heating Values, and the Energy Conservation Principle European Fuel Cell Forum, 29 October 2003. http://www.efcf.com/reports/E10.pdf.
[26] J. Larminie, A. Dicks, Fuel Cell Systems Explained, John Wiley & Sons, 2000, 247–248.